Available online at www.sciencedirect.com
ScienceDirect
Ceramics International 37 (2011) 701–706
CERAMICS INTERNATIONAL
www.elsevier.com/locate/ceramint

Microstructure and electrical properties of Sc_2O_3-doped ZnO–Bi_2O_3-based varistor ceramics

Dong Xu [a,b], Xiaonong Cheng [a,*], Guoping Zhao [a], Juan Yang [a], Liyi Shi [b]

[a] School of Material Science and Engineering, Jiangsu University, Zhenjiang 212013, China
[b] School of Material Science and Engineering, Shanghai University, Shanghai 200072, China

Received 17 November 2009; received in revised form 24 May 2010; accepted 25 September 2010
Available online 28 October 2010

Abstract

The microstructure and electrical properties of ZnO–Bi_2O_3-based varistor ceramics doped with different Sc_2O_3 content sintered at 1100 °C were investigated. The results showed that the nonlinear coefficient of the varistor ceramics with Sc_2O_3 were in the range of 18–54, the threshold voltage in the range of 250–332 V/mm, the leakage current in the range of 0.1–23.0 μA, with addition of 0–1.00 mol% Sc_2O_3. The ZnO–Bi_2O_3-based varistor ceramics doped with Sc_2O_3 content of 0.12 mol% exhibited the highest nonlinearity, in which the nonlinear coefficient is 54, the threshold voltage and the leakage current is 278 V/mm and 2.9 μA, respectively. The results confirmed that doping with Sc_2O_3 was a very promising route for the production of the higher nonlinear coefficient of ZnO–Bi_2O_3-based varistor ceramics, and determining the proper amounts of addition of Sc_2O_3 was of great importance.
© 2010 Elsevier Ltd and Techna Group S.r.l. All rights reserved.

Keywords: B. Microstructure-final; C. Electrical properties; D. ZnO; E. Varistors

1. Introduction

The zinc oxide based varistors are widely used in electronic appliances and especially in high voltage lines as voltage surge protection devices [1–5]. Commercial varistors are usually made by solid state of ZnO particles with doping agent oxides such as Bi_2O_3, Sb_2O_3, Co_2O_3, MnO_2 and Cr_2O_3, the mixed powder then being pressed and sintered at higher temperatures. Then a complex microstructure is achieved, in which conducting ZnO grains, an electrically insulating secondary spinel phase and a Bi-rich inter-granular phase are achieved.

To increase the threshold voltage, it is necessary to decrease the average size of the ZnO grains. It is clear that the addition of the rare-earth element decreases the diameter of ZnO grains and increases the varistor voltage [5–9]. However, a study of the effects of the new rare-earth oxides, Sc_2O_3 on the electrical properties of ZnO–Bi_2O_3-based varistor ceramics has been seldom reported. On the other hand, the traditional rare-earth oxide in ZnO–Bi_2O_3-based varistor ceramics had been used to improve the electrical characteristics of ZnO varistors, but the nonlinearity of ZnO varistor becomes bad [10].

In this paper, a new ceramic composition is proposed and consists in using a rare earth oxide: Sc_2O_3. The Sc_2O_3 effects on the microstructure and the electrical properties of the ZnO–Bi_2O_3-based varistor ceramics were investigated and some new results were obtained.

2. Experimental procedure

Reagent-grade raw materials were used in proportions of $(96.5 - x)$ mol% ZnO, 0.7 mol% Bi_2O_3, 1.0 mol% Sb_2O_3, 0.8 mol% Co_2O_3, 0.5 mol% Cr_2O_3, 0.5 mol% MnO_2, and x mol% Sc_2O_3, for $x = 0$, 0.02, 0.04, 0.12, 0.20, and 1.00 (samples labeled A0, A1, A2, A3, A4, and A5, respectively). After milling, the mixture was dried at 70 °C for 24 h, then the powder was uniaxially pressed into discs of 12 mm in diameter and 2 mm in thickness. The pressed disks were sintered in air at 1100 °C (2 h dwell time), using a heating rate of 5 °C/min and then cooled in the furnace. The sintered samples were lapped and polished to 1.0 mm thickness. The

* Corresponding author.
E-mail address: Frank@ujs.edu.cn (X. Cheng).

0272-8842/$36.00 © 2010 Elsevier Ltd and Techna Group S.r.l. All rights reserved.
doi:10.1016/j.ceramint.2010.09.032

final samples were about 10 mm in diameter and 1.0 mm in thickness. The bulk density of the samples was measured in terms of their weight and volume. For the characterization of DC current–voltage, the silver paste was coated on both faces of samples and the silver electrodes were formed by heating at 600 °C for 10 min. The electrodes were 5 mm in diameter. The voltage–current (V–I) characteristics were measured using a V–I source/measure unit (CJP CJ1001). The nominal varistor voltages (V_N) at 0.1 and 1.0 mA were measured [11–14] and the threshold voltage V_T (V/mm) ($V_T = V_N(1\text{ mA})/d$; d is the thickness of the sample in mm). The leakage current (I_L) was measured at $0.75V_N$ (1 mA). The measurement accuracy for voltage was ±0.5% and for electric current ±2%. In addition, the nonlinear coefficient α ($\alpha = 1/\log(V_{1.0\text{ mA}}/V_{0.1\text{ mA}})$) were determined with relative error of ±5% [12–19].

The crystalline phases were identified by an X-ray diffractometry (XRD, Rigaku D/max 2200, Japan) using a Cu Kα radiation. The surface microstructure was examined by a scanning electron microscope (SEM, FEI QUANTA 400). The average grain sizes (G) was determined by the linear intercept method, given by $G = 1.56L/MN$, where L is the random line length on the micrograph, M is the magnification of the micrograph, and N is the number of the grain boundaries intercepted by lines [20].

A Schottky-type barrier model is usually used to explain the behavior of varistors [21–23]. According to the model, the current density through a varistor is:

$$J = AT^2 \exp\left[\frac{(\beta E^{1/2} - \Phi_B)}{kT}\right] \quad (1)$$

where A is the Richardson constant, E is the electric field, k is the Boltzmann constant, T is the absolute temperature, and β is a constant related to the barrier width by the relationship:

$$\beta = \left[\left(\frac{1}{\gamma\omega}\right)\left(\frac{2e^3}{4\pi\varepsilon_0\varepsilon_r}\right)\right]^{1/2} \quad (2)$$

where γ is the number of grains per unit length, e is the electron charge (1.602×10^{-19} C), ε_0 is the vacuum dielectric constant (8.85×10^{-14} F/cm), and ε_r is the relative dielectric constant ($\varepsilon_r = 8.5\varepsilon_0$). By setting T at room temperature, and plotting $\ln J - E^{1/2}$ for samples, Φ_B can be obtained from the intersection of the extrapolated regression lines with the $\ln J$ axis, and the constant β can be derived from the slopes of the plots. Using the value of the β, the depletion layer width (ω) of either side at the grain boundaries is determined by Eq. (2). The donor density (N_D) can be estimated from the equation with relative error of ±2% [24,25].

$$\omega^2 = \frac{2\Phi_B\varepsilon_r\varepsilon_0}{e^2 N_D} \quad (3)$$

The density of the interface states (N_S) at the grain boundaries is determined by the equation:

$$N_S = N_D\omega \quad (4)$$

3. Results and discussion

The influence of the amount of addition of Sc_2O_3 on the characteristics, including the density ρ, the threshold voltage V_T, the nonlinear coefficient α, and the leakage current I_L of the ZnO–Bi_2O_3 varistors ceramic sintered at 1100 °C for 2 h is presented in Table 1. Doping with Sc_2O_3 also strongly influence the density of varistor ceramics, it is significant that the samples doped with various amounts of Sc_2O_3 have a higher density in comparison to the Sc_2O_3-free sample (5.47 g/cm^3). When Sc_2O_3 content is 0.02%, the maximum density is 5.60 g/cm^3. With increasing Sc_2O_3 contents the density changes slightly between 5.56 and 5.60 g/cm^3. When increasing Sc_2O_3 contents between 0.02 mol% and 0.20 mol%, the threshold voltage is lower than the original composition, while the threshold voltage increases when the content is 1.00 mol%. The result is agrees with the SEM results of the average ZnO grain size. The α of the varistor ceramics without Sc_2O_3 is only 30, whereas the α values of the varistor ceramics with Sc_2O_3 are in the range of 45–54, achieving maximum (54) in Sc_2O_3 content of 0.12 mol%, with the addition of 0.02–0.20 mol% Sc_2O_3. When the Sc_2O_3 content was higher than 0.20 mol%, the α value was decreased abruptly with increasing Sc_2O_3 content. It can be seen that the incorporation of Sc_2O_3 (0.02–0.20 mol %) can increase the α value greatly. The results are different with the reports of the early rare earth doped ZnO-based varistor ceramics.

Fig. 1 shows the electric field–current density (E–J) curves of ZnO–Bi_2O_3-based varistor ceramics with various Sc_2O_3

Table 1
Density and electrical properties of Sc_2O_3 doped ZnO–Bi_2O_3-based varistor ceramics.

Sample	ρ (g/cm^3)	I_L (μA)	V_T (V/mm)	α
A0	5.47	0.1	332	30
A1	5.59	0.7	260	51
A2	5.56	1.3	268	53
A3	5.60	2.9	278	54
A4	5.59	1.1	270	49
A5	5.60	23.0	310	18

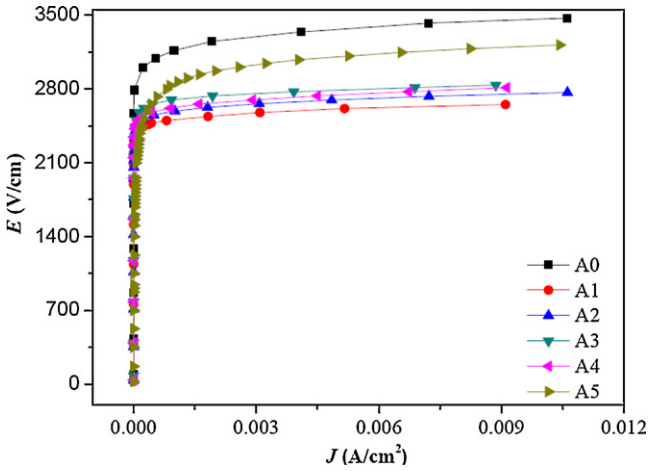

Fig. 1. E–J curves of ZnO–Bi_2O_3-based varistor ceramics doped with Sc_2O_3.

contents. The curves show that the conduction characteristics are divided into two regions: linear region before breakdown field and nonlinear region after breakdown field. The sharper the knee of the curves between the two regions is, the better the nonlinear properties are [7]. As it can be seen from Fig. 1, the knee region of E–J curves with Sc_2O_3 is much keener than that without Sc_2O_3. This clearly shows that the incorporation of Sc_2O_3 greatly improves the nonlinear properties of varistor ceramics. The varistor ceramics with Sc_2O_3 contents of 0.02 mol% and 0.20 mol% is assumed to exhibit similar characteristics because their curves are very closely adjoined. As adding more Sc_2O_3, the knee gradually becomes more pronounce and the nonlinear properties enhance. Therefore, the addition of Sc_2O_3 seems to enhance remarkably the nonlinear properties. The breakdown field decreases greatly in accordance with increasing Sc_2O_3 amount but when the Sc_2O_3 content is 1.00 mol%, it is nearly uniformly without Sc_2O_3. This phenomenon suggests that Sc_2O_3 can affect the breakdown voltage of a grain boundary significantly. The variation of E in accordance with increasing Sc_2O_3 amount could explain by the increase in the number of grain boundaries owing to the decrease of average ZnO grain size and the breakdown voltage of a grain boundary. All of these will have some influence on the electrical properties of varistor ceramics.

XRD patterns of the investigated samples are given in Fig. 2. No changes in crystal structure are observed in the samples. The sample without addition of Sc_2O_3 and the samples doped with various amounts of Sc_2O_3 also are composite materials, consisting typically of three phases: ZnO, spinel and an intergranular Bi-rich phase. The XRD peak intensities variety of the spinel phase and an intergranular Bi-rich phase with the variety Sc_2O_3 content, and have the relationship of the threshold voltage V_T, the nonlinear coefficient α. The Sc_2O_3 is not observed maybe because they only account for a small fraction of the overall composition, as has been reported previously [13]. Table 2 presents Sc_2O_3 doped on the relative X-ray diffraction peak area ratios, which indicated the different phase amount in the varistor ceramics, such as ZnO, spinel and Bi-rich phase. As can be seen form Table 2, when the Sc_2O_3 additive content is less than 0.04 mol%, the amount of pyrochlore phase have little change with increasing Sc_2O_3 additive content, in the same time, the amount of spinel phase increase with increasing Sc_2O_3 additive content. Moreover, when the Sc_2O_3 additive content is more than 0.04 mol%, the amount of pyrochlore phase have significantly increase with increasing Sc_2O_3 additive content, and the amount of spinel phase have a little increase relatively with increasing Sc_2O_3 additive content (Table 3).

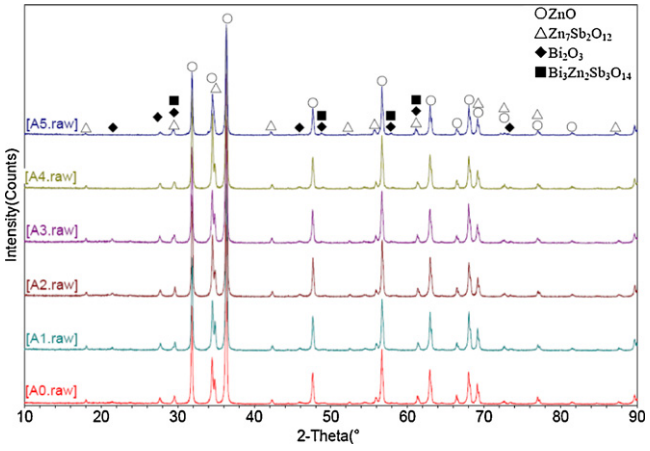

Fig. 2. XRD patterns of ZnO–Bi_2O_3-based varistor ceramics doped with Sc_2O_3.

Fig. 3 shows the SEM micrographs of the sample without addition of Sc_2O_3 and the samples doped with various amounts of Sc_2O_3 sintering at 1100 °C for 2 h. A similar microstructure of the samples obtains in all cases with the only appreciable differences coming from the average size of ZnO grains, maybe due to Sc_2O_3 had little effect on grain boundary migration of ZnO–Bi_2O_3-based varistors. In other words, there is no phase

Table 2
Effect of Sc_2O_3 doped on the relative X-ray diffraction peak area ratios.

Sample	Bi_2O_3(310)/ZnO(101)	$Bi_2Sb_3Zn_2O_{14}$(222)/ZnO(101)	$Zn_7Sb_2O_{14}$(311)/ZnO(101)
A0	0.040	0.047	0.237
A1	0.049	0.048	0.358
A2	0.046	0.047	0.393
A3	0.049	0.063	0.410
A4	0.046	0.053	0.459
A5	–	0.069	0.513

Table 3
Average grain sizes and boundary characteristics of ZnO–Bi_2O_3-based varistor ceramics doped with Sc_2O_3.

Sample	G (μm)	Φ_B (eV)	ω (nm)	N_D (10^{18} cm^{-3})	N_S (10^{12} cm^{-2})
A0	8.5	0.97	7.8	15.2	11.7
A1	9.1	0.96	7.8	14.7	11.5
A2	8.5	0.94	7.8	14.7	11.4
A3	8.1	0.96	6.4	22.2	14.1
A4	8.7	0.98	6.4	22.3	14.4
A5	7.5	0.89	8.3	12.2	10.1

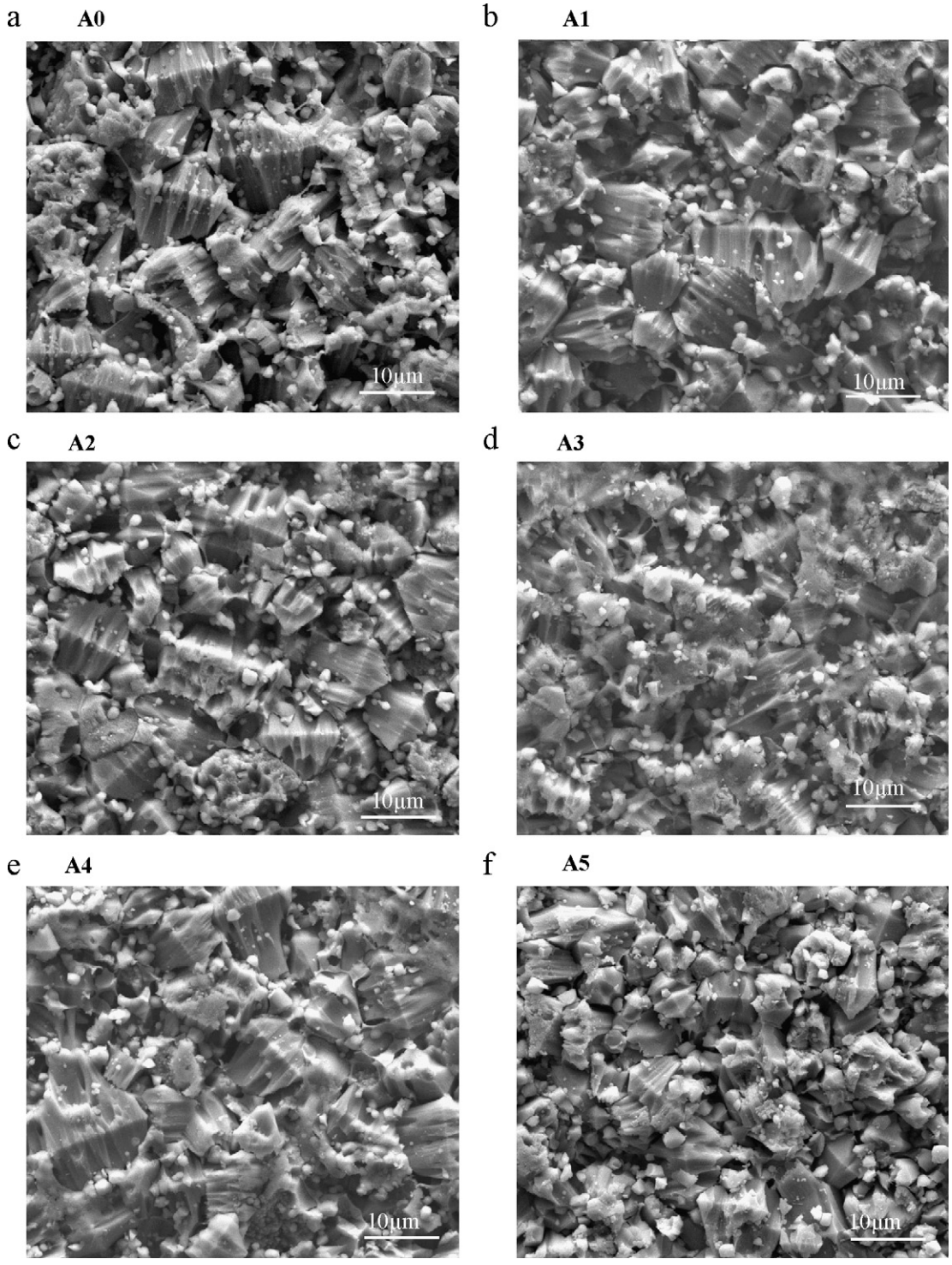

Fig. 3. SEM images of ZnO–Bi_2O_3-based varistor ceramics doped with Sc_2O_3.

change with the change of the amount of Sc_2O_3; it agrees with the results of Fig. 2. The sample A5 has a smaller average ZnO grain size than the other samples doped with Sc_2O_3. For the ZnO–Bi_2O_3-based varistors ceramics, the smaller the grains size, the higher the threshold voltage. Therefore, the threshold voltage of the sample A5 was higher than the other samples, and it is agrees with the results of Table 1.

Fig. 3 also shows the number of spinel have a significantly increase when the Sc_2O_3 additive content is 1.00 mol%, and it is according with the results of Table 2. Maybe with the increase of the spinel phase, the formation of ZnO–$Zn_7Sb_2O_{12}$ electrical active junctions increased the effective number of grain-boundaries, resulting in the increase of threshold voltage [13,26]. In the meantime, the spinel is a highly resistive phase,

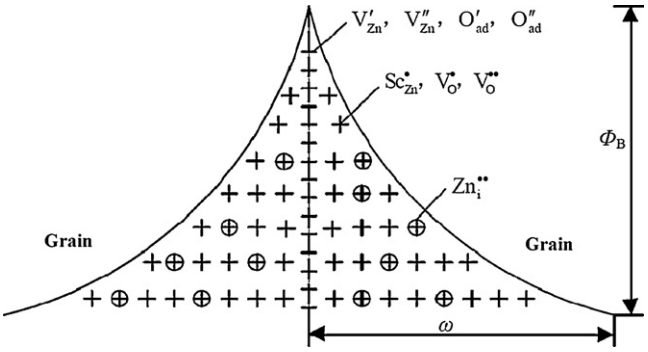

Fig. 4. Grain boundary defect model for ZnO–Bi_2O_3-based varistor ceramics doped with Sc_2O_3.

and ZnO–$Zn_7Sb_2O_{12}$ junctions do not contribute to the nonlinear effect [27], but on the other hand, maybe the more the junctions, the bad the uniform of the microstructure. Therefore, the nonlinear coefficient decreased and the leakage current increased.

The grain boundary properties of ZnO–Bi_2O_3-based varistor doped with Sc_2O_3 such as the donor concentration (N_D), the depletion layer width (ω), the density of interface states (N_S) and the barrier height (Φ_B) are presented in Table 2 and the defect barrier model are shown as Fig. 4. When the amount of Sc_2O_3 is less than 0.20 mol%, the donor concentration is increase slightly, the depletion layer width exhibited a tendency decreasing in the range of 6.4–7.8, and it is an opposite variation of the donor concentration. On the other hand, the density of interface states is increased and the barrier height is decreased with the increase of Sc_2O_3 content. The barrier height is directly associated with the donor concentration and density of interface states. Moreover, the barrier height is estimated by the variation rate in the density of interface states and donor concentration as represented expression (3, 4). Generally, the barrier height is increased with increasing density of interface states and decreasing donor concentration. If the variation rate of donor concentration is much larger than that of density of interface states with an additive content, the barrier height is much more strongly affected to donor concentration than density of interface states. According to this reason, it would be understood that the barrier height is increased or decreased with increasing Sc_2O_3 additive content [25,28]. In the same time, the depletion layer width increases and decreases also is associated with the increase and decrease of the donor concentration.

When the amount of Sc_2O_3 is more than 0.20 mol%, there may be some Sc_2O_3 phase inhibit the growth of ZnO grains by pinning effect. At the same time, the ZnO grain size decrease and the grain boundary increase, that is benefit for the formation of grain boundary phase. Therefore, with the increase of the amount of Sc_2O_3, the relative amount of Sc ion substitute into the ZnO lattice decrease and the donor concentration also decrease. On the other hand, in the conditions with the same adsorbed oxygen ions in the grain boundary, the grain refinement could lead to the grain boundary increase, that will make the concentration of adsorbed oxygen ions of the grain boundary decrease, that is, the density of interface states decrease.

4. Conclusions

The microstructure and electrical properties of ZnO–Bi_2O_3-based varistor ceramics doped with different Sc_2O_3 content were investigated. The results showed that the threshold voltage of the samples doped with Sc_2O_3 were lower than the Sc_2O_3-free sample. With the addition of 0.02–0.20 mol% Sc_2O_3, the nonlinear coefficient of the varistor ceramics doped with Sc_2O_3 were in the range of 45–54, achieving maximum (54) in Sc_2O_3 content of 0.12 mol%, that was very high than that of the sample undoped with Sc_2O_3. The XRD and SEM also showed that no phase transformations were observed in the samples. When the amount of Sc_2O_3 is less than 0.20 mol%, the donor concentration increase basically, and the depletion layer width exhibited a tendency decreasing. When the amount of Sc_2O_3 is more than 0.20 mol%, the donor concentration and the density of interface states decrease. The results confirmed that doping with Sc_2O_3 was a very promising route for the production of the higher nonlinear coefficient ZnO–Bi_2O_3-based varistor ceramics, and determining the proper amounts of addition of Sc_2O_3 was of great importance.

Acknowledgments

This work was financially supported by National Nature Science Foundation of China (50902061), China Postdoctoral Science Foundation funded project (20100471380), Leading Academic Discipline Project of Shanghai Municipal Education Commission (J50102), State Key Laboratory of Inorganic Synthesis and Preparative Chemistry of Jilin University (2011-22), Jiangsu University Undergraduate Practice-Innovation Training Project (2010002) and Universities Natural Science Research Project of Jiangsu Province (10KJB430002).

References

[1] D.R. Clarke, Varistor ceramics, J. Am. Ceram. Soc. 82 (3) (1999) 485–502.
[2] P. Duran, F. Capel, J. Tartaj, C. Moure, A strategic two-stage low-temperature thermal processing leading to fully dense and fine-grained doped-ZnO varistors, Adv. Mater. 14 (2) (2002) 137.
[3] C.W. Nahm, Effect of sintering temperature on varistor properties and aging characteristics of ZnO–V_2O_5–MnO_2 ceramics, Ceram. Int. 35 (7) (2009) 2679–2685.
[4] S. Bernik, G. Brankovic, S. Rustja, M. Zunic, M. Podlogar, Z. Brankovic, Microstructural and compositional aspects of ZnO-based varistor ceramics prepared by direct mixing of the constituent phases and high-energy milling, Ceram. Int. 34 (6) (2008) 1495–1502.
[5] M. Houabes, R. Metz, Rare earth oxides effects on both the threshold voltage and energy absorption capability of ZnO varistors, Ceram. Int. 33 (7) (2007) 1191–1197.
[6] S. Bernik, S. Macek, B. Ai, Microstructural and electrical characteristics of Y_2O_3-doped ZnO–Bi_2O_3-based varistor ceramics, J. Eur. Ceram. Soc. 21 (10–11) (2001) 1875–1878.
[7] C.W. Nahm, Effect of sintering temperature on nonlinear electrical properties and stability against DC accelerated aging stress of (CoO,

Cr_2O_3 La_2O_3)-doped ZnO–Pr_6O_{11}-based varistors, Mater. Lett. 60 (28) (2006) 3311–3314.
[8] H.Y. Liu, H. Kong, D.M. Jiang, W.Z. Shi, X.M. Ma, Microstructure and electrical properties of Er_2O_3-doped ZnO-based varistor ceramics prepared by high-energy ball milling, J. Rare Earth 25 (1) (2007) 120–123.
[9] C.W. Nahm, C.H. Park, Effect of Er_2O_3 addition on the microstructure, electrical properties, and stability of Pr_6O_{11}-based ZnO ceramic varistors, J. Mater. Sci. 36 (7) (2001) 1671–1679.
[10] J.L. He, J. Hu, Y.H. Lin, ZnO varistors with high voltage gradient and low leakage current by doping rare-earth oxide, Sci. China Ser. E 51 (6) (2008) 693–701.
[11] Z.H. Wu, J.H. Fang, D. Xu, Q.D. Zhong, L.Y. Shi, Effect of SiO_2 addition on the microstructure and electrical properties of ZnO-based varistors, Int. J. Miner. Metall. Mater. 17 (1) (2010) 86–91.
[12] D. Xu, X. Cheng, M. Wang, L. Shi, Microstructure and electrical properties of La_2O_3-doped ZnO–Bi_2O_3-based varistor ceramics, Adv. Mater. Res. 79–82 (2009) 2007–2010.
[13] D. Xu, L. Shi, Z. Wu, Q. Zhong, X. Wu, Microstructure and electrical properties of ZnO–Bi_2O_3-based varistor ceramics by different sintering processes, J. Eur. Ceram. Soc. 29 (9) (2009) 1789–1794.
[14] D. Xu, L.Y. Shi, X.X. Wu, Q.D. Zhong, Microstructure and electrical properties of Y_2O_3-doped ZnO–Bi_2O_3-based varistor ceramics, High Voltage Eng. 35 (9) (2009) 2366–2370.
[15] S. Bernik, N. Daneu, Characteristics of ZnO-based varistor ceramics doped with Al_2O_3, J. Eur. Ceram. Soc. 27 (10) (2007) 3161–3170.
[16] S. Bernik, S. Macek, A. Bui, The characteristics of ZnO–Bi_2O_3-based varistor ceramics doped with Y_2O_3 and varying amounts of Sb_2O_3, J. Eur. Ceram. Soc. 24 (6) (2004) 1195–1198.
[17] C. Leach, Z. Ling, R. Freer, The effect of sintering temperature variations on the development of electrically active interfaces in zinc oxide based varistors, J. Eur. Ceram. Soc. 20 (16) (2000) 2759–2765.
[18] M. Peiteado, J.F. Fernandez, A.C. Caballero, Varistors based in the ZnO–Bi_2O_3 system: microstructure control and properties, J. Eur. Ceram. Soc. 27 (13–15) (2007) 3867–3872.
[19] D. Xu, X. Cheng, X. Yan, H. Xu, L. Shi, Sintering process as a relevant parameter for Bi_2O_3 vaporization from ZnO–Bi_2O_3-based varistor ceramics, Trans. Nonferr. Met. Soc. 19 (6) (2009) 1392–1399.
[20] C.W. Nahm, Effect of cooling rate on degradation characteristics of ZnO·Pr_6O_{11}·CoO·Cr_2O_3·Y_2O_3-based varistors, Solid State Commun. 132 (3–4) (2004) 213–218.
[21] C.W. Nahm, Effect of MnO_2 addition on microstructure and electrical properties of ZnO–V_2O_5-based varistor ceramics, Ceram. Int. 35 (2) (2009) 541–546.
[22] M. Matsuoka, Nonohmic properties of zinc oxide ceramics, Jpn. J. Appl. Phys. 10 (6) (1971) 736–746.
[23] C.W. Nahm, Microstructure and electrical properties of Tb-doped zinc oxide-based ceramics, J. Non-Cryst. Solids 353 (30–31) (2007) 2954–2957.
[24] H.Y. Liu, X.M. Ma, D.M. Jiang, W.Z. Shi, Microstructure and electrical properties Y_2O_3-doped ZnO-based varistor ceramics prepared by high-energy ball milling, J. Univ. Sci. Technol. B 14 (3) (2007) 266–270.
[25] W.X. Wang, J.F. Wang, H.C. Chen, W.B. Su, B. Jiang, G.Z. Zang, C.M. Wang, P. Qi, Varistor properties of Sc_2O_3-doped Sn·Co·Nb ceramics, Ceram. Int. 31 (2) (2005) 287–291.
[26] J.C. Zhang, S.X. Cao, R.Y. Zhang, L.M. Yu, C. Jing, Effect of fabrication conditions on *I–V* properties for ZnO varistor with high concentration additives by sol-gel technique, Curr. Appl. Phys. 5 (4) (2005) 381–386.
[27] N.T. Hung, N.D. Quang, S. Bernik, Electrical and microstructural characteristics of ZnO–Bi_2O_3-based varistors doped with rare-earth oxides, J. Mater. Res. 16 (10) (2001) 2817–2823.
[28] C.W. Nahm, C.H. Park, Microstructure, electrical properties, and degradation behavior of praseodymium oxides-based zinc oxide varistors doped with Y_2O_3, J. Mater. Sci. 35 (12) (2000) 3037–3042.